HAL
open science

CO2-Expanded alkyl acetates: physicochemical and molecular modeling study and applications in chemical processes

Emanuel Granero-Fernandez, Devin Machin, Corinne Lacaze-Dufaure, Séverine Camy, Jean-Stéphane Condoret, Vincent Gerbaud, Paul Charpentier, Yaocihuatl Medina-González

To cite this version:

Emanuel Granero-Fernandez, Devin Machin, Corinne Lacaze-Dufaure, Séverine Camy, Jean-Stéphane Condoret, et al.. CO2-Expanded alkyl acetates: physicochemical and molecular modeling study and applications in chemical processes. ACS Sustainable Chemistry & Engineering, 2018, 6 (6), pp.7627-7637. 10.1021/acssuschemeng.8b00454 . hal-01808278

HAL Id: hal-01808278

https://hal.science/hal-01808278v1

Submitted on 5 Jun 2018

HAL is a multi-disciplinary open access archive for the deposit and dissemination of scientific research documents, whether they are published or not. The documents may come from teaching and research institutions in France or abroad, or from public or private research centers.

L'archive ouverte pluridisciplinaire **HAL**, est destinée au dépôt et à la diffusion de documents scientifiques de niveau recherche, publiés ou non, émanant des établissements d'enseignement et de recherche français ou étrangers, des laboratoires publics ou privés.

Open Archive TOULOUSE Archive Ouverte (OATAO)
OATAO is an open access repository that collects the work of Toulouse researchers and makes it freely available over the web where possible.

This is an author-deposited version published in: http://oatao.univ-toulouse.fr/
Eprints ID: 20125

To link to this article: DOI: 10.1021/acssuschemeng.8b00454
URL: http://doi.org/10.1021/acssuschemeng.8b00454

To cite this version: Granero-Fernandez, Emanuel and Machin, Devin and Lacaze-Dufaure, Corinne and Camy, Séverine and Condoret, Jean-Stéphane and Gerbaud, Vincent and Charpentier, Paul and Medina-González, Yaocihuatl *CO2 - Expanded alkyl acetates: physicochemical and molecular modeling study and applications in chemical processes*. (2018) ACS Sustainable Chemistry and Engineering, vol. 6. pp. 7627-7637

Any correspondence concerning this service should be sent to the repository administrator: staff-oatao@listes-diff.inp-toulouse.fr

CO_2-Expanded Alkyl Acetates: Physicochemical and Molecular Modeling Study and Applications in Chemical Processes

Emanuel Granero-Fernandez,[†] Devin Machin,[§] Corinne Lacaze-Dufaure,[‡] Séverine Camy,[†] Jean-Stéphane Condoret,[†] Vincent Gerbaud,[†] Paul A. Charpentier,[§] and Yaocihuatl Medina-Gonzalez*,[†]

[†]Laboratoire de Génie Chimique, Université de Toulouse, CNRS, INPT, UPS, 4 Allée Emile Monso, CS 84234, 31030 Toulouse, France

[‡]CIRIMAT, Université de Toulouse, CNRS, INPT, UPS, 4 Allée Emile Monso, BP44362, 31030 CEDEX 4 Toulouse , France

[§]Department of Chemical and Biochemical Engineering, Western University, London, Ontario N6A 5B9, Canada

ABSTRACT: Different physicochemical properties of CO_2-expanded alkyl acetates (methyl, ethyl, propyl, and isoamyl acetates) have been studied by experimental and molecular modeling methods. Changes in the π^* Kamlet−Taft parameter with CO_2 pressure were determined by UV−vis spectroscopy by following the hypsochromic shift of Nile Red. Modeling of the systems by molecular dynamics (MD) and equation of state (EoS) methods to assess physical equilibrium, density, and viscosity were performed in order to fully characterize these media with the aim to control the physicochemical properties of these phases by pressure and temperature. The studied expanded phases were used in the fabrication of TiO_2 microparticles and the morphological properties measured. It is clear from this study that density, viscosity, and polarity of the expanded phase plays a key role in the morphological properties of the particles obtained. On the basis of these results, we propose these green media and CO_2 pressure as a way to control the properties of semiconductor microparticles.

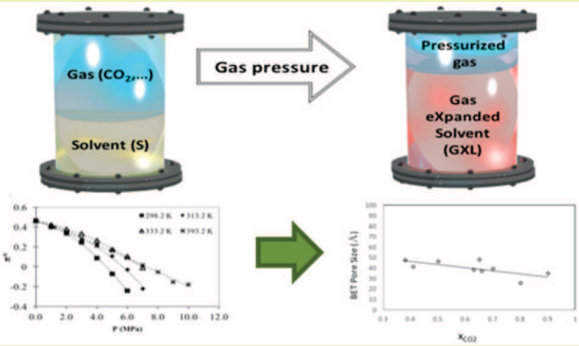

KEYWORDS: *Gas-expanded liquids, Alkyl acetates, Green solvents, Biosourced solvents, Solvent properties*

INTRODUCTION

Gas-expanded liquids (GXLs) are liquids whose volume is expanded by a pressurized dissolved gas. The dissolution of the gaseous compound and the expansion of the liquid phase lead to changes in the physicochemical and transport properties of the new expanded phase. This expanded phase can contain high concentrations of CO_2 (up to 80%, depending on the solvent), which can lead to an effective reduction of the need for organic solvent, providing better transport properties than organic liquids.[1,2]

A number of properties of GXLs, including solvation properties, can be tuned by addition of CO_2 to the liquid solvent,[3] which then becomes a tool to modify the physicochemical and transport properties of the liquid solvent. Concerning solubility, for example, solutes that are soluble in CO_2-expanded solvents may precipitate when CO_2 is removed. On the contrary, if a solute is highly soluble in a solvent, the addition of CO_2 can induce its precipitation. The cybotactic region in GXLs, which is the volume surrounding a solute molecule, where the local solvent structure plays a key role in solubility and transport phenomena and is strongly influenced by intermolecular forces between the solvent and the solute, characterized by local composition and density, can be used to optimize reactions and separation. This optimization is possible if the local solvent structure changes with CO_2 concentration are well understood.[4,5]

Recently, the importance of taking into account solvent effects on the performance of chemical processes has been emphasized.[4,6−8] As a case study, a model for the integrated design of a GXL for a given reaction and the conceptual design of the associated reactor-separation system has been developed, and the best GXL was chosen on the basis of the overall economic performance of the process. An empirical model correlating the reaction rate constant to solvent solvation properties was used in the calculation of the performance of the chemical process.[9]

Alkyl acetates are solvents widely used in research and in industry and generally considered as green, and nontoxic or biodegradable, particularly ethyl acetate, which is authorized for pharmaceutical and cosmetic applications.[10] In the work presented here, the properties of CO_2-expanded alkyl acetates have been studied by spectroscopic measurements and by MD calculations. In this context, even if different scales can be used to characterize and quantify solvent properties, the Kamlet−Taft

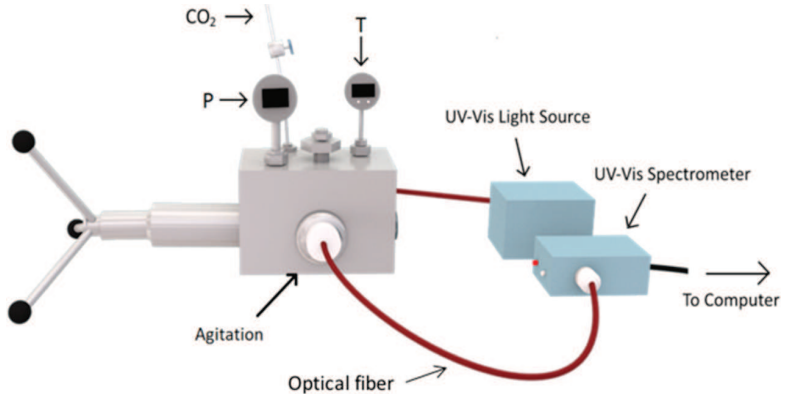

Figure 1. Experimental setup used for solvatochromic determinations; phase equilibria determinations have been performed visually by using the same variable-volume high-pressure cell.

parameters[11] have been selected for this work as they have been used in previous studies to effectively describe solvent effects in organic solvents and gas expanded liquids.[12−14] The π^* Kamlet−Taft parameter of the expanded phase has been determined in this study by UV−vis spectroscopic measurements, and vapor−liquid equilibrium has been determined experimentally and numerically by using the Soave−Redlich−Kwong Equation of State (SRK EoS). Density and viscosity of these GXLs have been studied by MD, which is a technique allowing the accurate prediction of physicochemical properties of an expanded phase if the correct force field is used.[15−18] In particular, density results obtained by MD have been compared with literature data when available.

In this study, we propose to assess the impact of the control of the physicochemical properties of CO_2-expanded alkyl acetates in the process of preparing TiO_2 microparticles (μPs) in these solvents and on the morphology of the obtained microparticles. Indeed, the properties of the solvent used during the μPs synthesis is known to strongly influence the kinetics of nucleation, growth, coarsening, and aggregation. Particle properties such as size, optical bandgap, and in general growth kinetics are strongly influenced by solvent properties such as polarity, viscosity, surface tension, and so on.[19,20] Our study shows that control of the solvency and transport properties allows control on BET pore size and specific surface area of the TiO_2 μPs obtained, which is key to tailor optical, electrical, chemical, and magnetic properties of these microparticles for specific applications such as catalysis, formulation, and so forth

■ MATERIALS AND METHODS

Carbon dioxide (>99% purity) was supplied by Air Liquid. Methyl Acetate (>95%), Ethyl acetate (99.5%), propyl acetate (99%), and isoamyl acetate (>95%) were obtained from Sigma-Aldrich and were used as received.

The phase equilibria and polarity measurements were performed by using the experimental equipment used in our previous studies.[21] Briefly, a high-pressure variable-volume view cell (9.6-31.3 cm^3, Top Industrie, France) equipped with three sapphire windows and a magnetic stirrer (Figure 1) and a 260D high-pressure Teledyne Isco syringe pump (the precision of the injected volume is ±1 cm^3). The temperature of the cell was kept at the desired value by a thermostatic bath and measured by a thermocouple (J type, precision of ±0.1 K) placed inside of the cell. Pressure was measured by a digital manometer (Keller, LEX 1, precision: 0.01%). For polarity measurements, optical fibers were used to perform the in situ measurements by using a StellarNet Inc. EPP2000 CCD UV−vis spectrophotometer and an Ocean Optics DH-2000 light source.

Experimental Determinations. *Phase Equilibrium.* Phase equilibrium data is necessary to understand the physicochemical properties of gas-expanded liquids. In this study, vapor−liquid equilibria (VLE) data was needed in order to know the composition of the expanded phases at any temperature and pressure. Some VLE data for systems containing alkyl acetates and CO_2 have been reported in the literature.[22−32] However, specific data needed for the study presented here had to be determined experimentally and/or calculated by MD techniques or by using an equation of state, such as VLE at temperatures not yet reported, densities, and CO_2 molar fraction in the expanded phase. Bubble curves have been obtained by the following procedure. A known volume, usually 10.0 mL, of alkyl acetate at the evaluated temperature was loaded in the high-pressure cell (Figure 1). Alkyl acetate volumes were measured with a brand new, calibrated, 10 mL micropipette PIPETMAN from Gilson, whose accuracy is reported as ±60 μL. The air contained in the cell was removed by decreasing the volume to its minimum to reduce as possible the presence of other compounds in the cell such as N_2 from air. The air contained inside the cell was then considered as negligible. The cell was then closed, and a known volume of CO_2 was pumped into the cell at known temperature and pressure by using a syringe pump, allowing to know the exact volume of CO_2 injected. Pressure inside the cell was carefully controlled by using the piston of the cell. The total composition inside of the cell was then known. The mixture was initially equilibrated at the desired temperature as a two-phase system. At that point, the system was pressurized with the piston to transform the system from two phases into a single-phase system. The system was then depressurized by opening the piston until a second phase was visible. Compression and decompression operations were repeated to obtain the narrowest range of pressures for the phase transition. Temperatures studied were between 298.2 and 393.2 K, and the relative pressure was varied from 0 to 14.7 MPa.

Solvatochromic Determinations. For GXLs, the Kamlet−Taft parameters (KT)[11,33−35] present great interest to give an idea of the acidity (α, ability to donate a proton in a solvent−solute hydrogen bond), the basicity (β, ability to accept a proton in a solvent−solute hydrogen bonding), and the dipolarizability (π^*, ability to stabilize a charge or dipole) of the expanded phase. These parameters had been used previously to study solvent effects in other GXLs.[1,12,36−40]

Experimental determinations of KT parameters are based on solvatochromism, which is the effect induced by the solvent molecules on the wavelength of maximal absorption of certain indicators.[41] Nile Red (NR) has been used before[42] as a solvatochromic molecule as it presents a large shift in its absorption maxima. When the polarity of the solvent increases, the absorbance spectra show a bathochromic shift.[43] Inversely, when polarity decreases, Nile Red presents a hypsochromic shift. The relation between this shift and dipolarizability parameter has been reported in literature[44,45] for hydrogen bonding donor solvents (HBD) and non-hydrogen bonding solvents (NHD, α parameter = 0); for the case of alkyl acetates (NHB), this parameter can be calculated from eq 1[44]

$$\lambda_{max} = 19993 - 1725^{*}\pi^{*} \quad (1)$$

where λ_{max} is expressed in the energy unit kiloKaiser (kK), in order to convert the wavelength into wavenumber. The π^* parameter is dimensionless.

Solvatochromic determinations were performed as follows: the selected alkyl acetate was added to the high-pressure cell, and a reference spectrum was obtained. After this, NR was added to an appropriate concentration, so the absorbance peak was clearly visible, and then the cell was flushed with CO_2 and tightly closed. The temperature was maintained by the thermostatic bath, and the content was stirred by a magnetic bar. CO_2 was then injected to the desired pressure. UV−vis spectra of the NR in the GXL phase were recorded. Physical equilibrium was considered to be reached when the pressure were constant for at least 1 h.

Modeling by Soave−Redlich−Kwong Equation of State (EoS). Phase equilibrium and expanded-phase density calculations of CO_2-alkyl acetates binary systems at temperatures ranging from 298.15 to 393.15 K were performed by using the well-known Soave−Redlich−Kwong Equation of State (EoS)[46] with the modification from Boston and Mathias for compounds above their critical temperature.[47] Classical van der Waals one-fluid mixing rule (vdW 1f) were used for calculation of *a* and *b* parameters of SRK-BM EoS, with standard combining rules, i.e., geometric rule with k_{ij} binary interaction coefficient for a_{ij} parameter and arithmetic mean rule without any coefficient for b_{ij} parameter. Literature data have been fitted with SRK-BM EoS in order to determine binary interaction parameters necessary for each binary system. Calculations have been performed by using Simulis Thermodynamics software (ProSim S.A. France).

Molecular Modeling (MM). Molecular dynamics was used to calculate the density and viscosity of the expanded phase. For these calculations, a box containing a given number of CO_2 and alkyl acetate molecules, at composition fixed by the physical equilibrium, was considered at fixed T and P. The composition of the liquid phase at equilibrium was obtained from literature[22,24,26−28,30−32] and from our own determinations in this work (section 2.1.1).

MD potentials were selected from those available in the Materials Processes and Simulations (MAPS) Suite from Scienomics[48] and in the Large-scale Atomic/Molecular Massively Parallel Simulator (LAMMPS) code from Sandia National Laboratories.[49] After several tests, the "Amber Cornell Extended" force field shown in Table S1 was chosen, which includes the Harris and Yund model for the CO_2 molecule. The method used for these calculations were similar to those used in our previous works.[50]

For viscosity calculations, the fluctuation−dissipation theorem explains how transport coefficients associated with irreversible processes can be described using reversible microscopic fluctuations.[51] Green−Kubo[52,53] relations give the mathematical expression for transport coefficients in terms of integrals of time-correlation functions.

In the standard Green−Kubo method, the dynamic (shear) viscosity of a fluid can be calculated by integrating the autocorrelation function of the stress tensor over time (eq 2):

$$\eta = \frac{V}{k_B T} \lim_{\tau \to \infty} \int_0^{\tau} P_{xy}(t) P_{xy}(0) \mathrm{d}t \quad (2)$$

where $\langle P_{xy}(t) P_{xy}(0) \rangle$ is the correlation function of the *xy* component of the stress tensor, V is the volume of the simulation box, k_B is the Boltzmann constant, T is the absolute temperature, and t is the time.

The geometries of all alkyl-acetates molecules were optimized at the DFT/6-31+G** level using the B3LYP functional (Gaussian09[54]). The partial charges were determined fitting the electrostatic potential according to the Merz−Singh−Kollman scheme.[55,56] The ESP charges obtained are shown in Table S2.

The sum of all atom charges was zero, so there was no global charge in the cell.

The simulated boxes were set with periodic boundaries in all directions containing a total of 1000 molecules in the NPT ensemble. A typical simulation box is shown in Figure S2. This box size was found to be the best compromise between a cell large enough for minimize the volume effects and small enough for an efficient computational calculation time. The simulations were performed as follows: NPT equilibration and density production runs of 1 200 000 steps. After that, equilibration runs in the canonical ensemble (NVT) were performed for 400 000 steps, followed by microcanonical ensemble (NVE) production runs for viscosity during 1 200 000 steps. All runs were performed with a time step of 1 fs. The L-J and Coulombic cutoff was set to 8 Å with a switching distance of r = 12 Å. Long-range interactions were calculated with the PPPM method. The simulations were started with randomly assigned velocities, the total momentum of the system was set to zero, and Newton's equations of motion were solved with the standard Velocity-Verlet algorithm. Calculations were performed by using the EOS supercomputer of CALMIP.

Effect of the Modulation of Solvent Properties in Morphology of TiO_2 Microparticles. To exemplify the impact of physicochemical properties control in CO_2-expanded alkyl acetates by pressure, TiO_2 microparticles (μPs) were prepared in CO_2-expanded ethyl and isoamyl acetates. Indeed, kinetics of nucleation, aggregation, coarsening, and growth, are expected to greatly depend on the properties of the solvent used for the synthesis of μPs.

TiO_2 μPs were synthesized in a high-pressure view-cell. The high-pressure cell contained a CO_2 inlet as well as temperature and pressure controllers. A syringe pump was used to deliver the pressurized CO_2 into the view cell. Titanium butoxide (TBO, 97%, Sigma-Aldrich) was used as precursor. Ethyl acetate (EA, 99,5%, Sigma-Aldrich) and isoamyl acetate (IA, 99,5%) were used together with $scCO_2$ (>99%) at several conditions of pressure and temperature. Detailed information about the experimental conditions is reported in Table 1. The reaction volumes were limited to 35 mL to accommodate the maximum internal volume capacity of the reactor. All chemicals were used as received.

Table 1. Reaction Conditions for TIO_2 μPs Fabrication in CO_2-Expanded Alkyl Acetates[a]

	solvent	T (K)	P (MPa)
(a)	EA	323.2	5.0
(b)	EA	353.2	5.0
(c)	EA	353.2	10.0
(d)	EA	373.2	10.0
(e)	IA	353.2	5.0
(f)	IA	353.2	10.0
(g)	IA	373.2	5.0
(h)	IA	373.2	10.0
(i)	IA	373.2	15.0

[a]EA = ethyl acetate, IA = isoamyl acetate.

In a typical reaction run, the reactants were added into the view cell all at once. The mixture was heated to the desired temperature, after which CO_2 was pumped into the cell until the desired pressure was reached. Reactant volumes were approximately 20 mL, and the remaining volume of the reactor was left for CO_2. The reactions were conducted for 3 h under constant stirring.

For all samples, the solvent was evaporated in an oven overnight at 60 °C

The as-prepared TiO_2 powders were amorphous but readily converted to crystalline anatase by calcination, during 4 h at 400 °C. The obtained materials were characterized by N_2 physisorption using a Micromeritics TriStar II 3020 instrument and by SEM in order to study the morphological characteristics.

RESULTS

Fluid-Phase Equilibria. In order to correctly model the physicochemical properties of expanded phase by MD, physical equilibrium data were needed. Although VLE determinations for CO_2-expanded alkyl acetate systems have been reported in the literature,[22,24−32,57−59] some of the data needed for our work were not available. Experimental determinations were performed using the visual method described in previous sections for the

Table 2. Calculated k_{ij} from Literature Data[27,31] and Corresponding AARD on CO_2 Mole Fraction in Liquid Phase

binary system	temperature range	number of points	k_{ij}	$\%AARD_{xCO_2}$
CO_2/methyl acetate	[313.2−393.2] K	64	0.1823−0.00065T	3.33
CO_2/ethyl acetate	[313.2−393.2] K	74	0.1524−0.00048T	6.14
CO_2/propyl acetate	[313.2−393.2] K	66	0.2993−0.00084T	0.03
CO_2/isoamyl acetate	[313.2−333.2] K	30	0.1391−0.00049T	1.54

alkyl acetates at temperatures where literature data were not found, i.e., all CO_2-alkyl acetates at 298.2 K and CO_2-isoamyl acetates at 393.2 K. Literature data[27,31] have been fitted using SRK EoS as described previously, and resulting binary interaction parameters are reported in Table 2. Absolute average relative deviation (eq 3) on CO_2 liquid mole fraction (x_{CO_2}) is also provided.

$$\%AARDx_{CO_2} = \frac{1}{N_p}\sum_{i=1}^{Np}\left|\frac{x_{CO_2}^{exp} - x_{CO_2}^{calc}}{x_{CO_2}^{exp}}\right| \times 100 \quad (3)$$

Figure 2 shows experimental VLE results for some conditions not available in the existing literature, along with literature data and EoS modeling results. Binary interactions parameters shown in Table 2 for SRK calculations were fitted to literature data as described in the section Experimental Determinations, but not to our own experimental determinations. This can be appreciated in the graphics as the SRK calculations show a better agreement to literature data (fitted) than to experimental values (not fitted). In Figure 2, both experimental and literature values are given for the CO_2-expanded alkyl acetates studied at different temperatures, in order to validate our experimental methodology, and results obtained from EoS are presented as well. The binary interactions parameters were fitted by using one or more temperatures in order to better predict the phase behavior for temperatures where no literature or experimental data is available. A maximal difference between our experimental values and those predicted by SRK is lower than 0.5 MPa. This difference can be appreciated at higher temperatures (Figure 2d).

Solvatochromic Determinations. Normalized absorption spectra of NR in CO_2-expanded ethyl acetate at different pressures and at 313.2 K are shown in Figure S3. This figure shows the typical behavior of NR in neat and CO_2-expanded alkyl acetates. NR absorbance spectra consist of one peak in the visible region. The shape of the peak remains unchanged at all pressures, but it undergoes a hypsochromic shift as the result of the increasing CO_2 mole fraction in the expanded phase.

Nile Red is a solvatochromic molecule whose absorbance undergoes a hypsochromic shift when the polarity of the surrounding medium decreases.[42,60,61] However, NR also undergoes a shift as a result of temperature effect, and this behavior is called thermochromism. The effect of the temperature in the maximal absorption wavelength of Red Nile at P_{atm} is shown in Figure S3. The thermochromic effect for NR gives a linear relation in the four neat acetates for the range of temperatures studied. Previous studies[62] on NR thermochromic behavior were performed on other solvents, and in all cases a linear relation was obtained. To avoid misinterpretation of absorption shifts observed during UV−vis determinations, the linear relation was used to correct the obtained values by using eq 1. Corrected Kamlet−Taft π^* parameter values are shown in Table S3 for the four alkyl acetates studied at different pressures for temperatures from 298.2 to 393.2 K; these results are depicted in Figure 3.

π^* parameter of CO_2-expanded alkyl acetates clearly decreases with pressure, as CO_2 concentration in the mixture increases. In Table S4, π^* parameter values for other commonly used solvents are presented.[13] As it can be observed, CO_2 pressure allows changes in π^* parameter of the mixture in a wide range of values, going from those of toluene or ethanol to that of linear alkanes such as *n*-pentane.

Molecular Modeling of CO_2-Expanded Acetates. Calculated liquid density and standard deviation values for the four CO_2-expanded alkyl acetates studied at 298.2, 313.2, 333.2, and 393.2 K are shown in Table S5 for absolute pressures from 1 to 12 MPa; these results are depicted in Figure 4, along with some literature data obtained experimentally. At low temperatures, two distinct zones can be observed: low and high pressure zones. First, at low pressure, density slightly increases as the CO_2 solubilizes, and this increase is more evident at low temperatures (see table S5). Then, above a certain pressure, the high CO_2 mole fraction produces a drastic volume increase and as a consequence a decrease in density.

At high temperatures, especially at 393.2 K, the density does not seem to increase significantly or even remains constant in the low-pressure zone. Nevertheless, density still decreases abruptly after reaching a certain point in the high-pressure zone; the point of strong density decrease depends on both alkyl chain length and temperature.

This behavior observed concerning density and expansion can be explained by an increase in free volume observed in GXLs[40] that has been attributed to the intermolecular spaces of the solvent that can host the CO_2 to some extent ($x_{CO_2} \approx 0.7$), increasing the density of the mixture; after this point, interstices between solvent molecules cannot receive any more CO_2, and thus the mixture experiences a rapid volume expansion.[40,63] The amount of CO_2 that the system can accommodate highly depends on temperature, as the gas solubility decreases and the molecular mobility increases.

Values obtained by MD are in a good agreement with experimental literature values for the CO_2-expanded methyl, ethyl and propyl acetate systems at 313.2 K. It can be observed that an increase in the alkyl acetate hydrocarbon chain length, caused a more pronounced increase in density at low concentrations of CO_2, which means that more CO_2 molecules can be accommodated in the interspaces formed by longer molecules than in the case of shorter hydrocarbon chains. Aida and colleagues[24] concluded, from an analysis of volume expansion in CO_2 + alkyl acetate systems and data from Peng−Robinson EoS, that the partial molar volume of acetates is higher for longer alkyl chain lengths, meaning that interspaces increase with increasing alkyl chain lengths.

In order to support these results, the packing fraction (f_{OCC}) has been calculated as the relation between the constituent molecules Van der Waal's volume as the sum of atomic radii[64] and the total volume of the simulated box. The f_{OCC} values are shown in Figure S4.

The observed behavior of calculated f_{OCC} gives an idea about the molecular order under the evaluated conditions. As it can be observed, f_{OCC} decreases monotonically, and after a certain composition, the CO_2 molecules have less free available space around the alkyl acetates molecules and the addition of CO_2

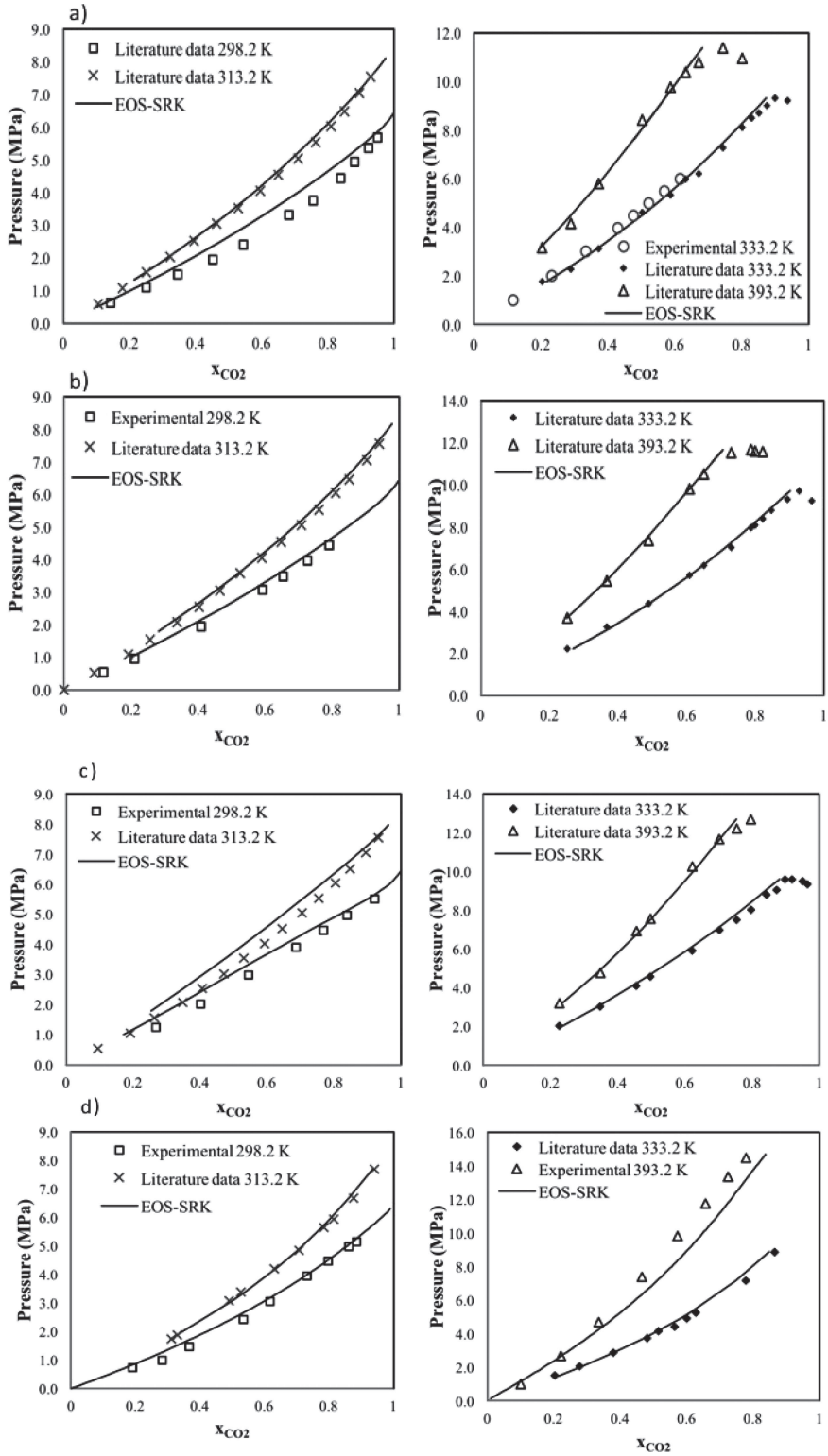

Figure 2. VLE experimental, literature, and EoS calculations curves for (a) methyl acetate; (b) ethyl acetate; (c) propyl acetate; and (d) isoamyl acetate at different temperatures.

causes a more pronounced fall of f_{OCC}. As it has been previously stated,[62] GXLs are fluids with more free volume than the pure liquids, which contributes to their increased transport properties already observed.[63] Higher f_{OCC} are observed in isoamyl acetate than for the other alkyl acetates at the same x_{CO_2}, which can be explained by the fact that interspaces in branched alkanes are occupied in part by the branched alkyl groups leaving less free volume between molecules.

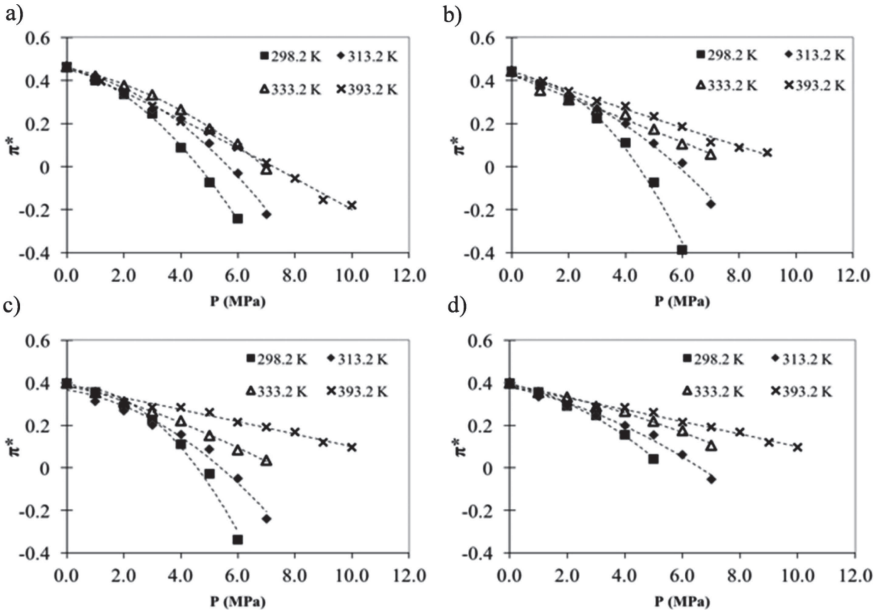

Figure 3. Corrected values of π^* as a function of pressure for (a) methyl, (b) ethyl, (c) propyl, and (d) isoamyl acetates expanded by CO_2.

Results obtained for viscosity from MD calculations at different pressures and temperatures of 298.2K to 393.2K for the systems studied are presented in Figure 5.

The calculated standard deviation for calculated viscosity for all the systems studied falls under 5×10^{-10}. The calculated viscosities behavior is coherent with values previously reported for CO_2-expanded systems,[65] calculated by molecular dynamics. In these systems, the viscosity decreases as a quasi linear function of CO_2 mole fraction. This behavior has been observed before in experimental data of ionic liquids, polymers, and crude oils when expanded by CO_2. In the case of alkyl acetates, it can be explained by the decrease of electrostatic forces between the solvent molecules because of the interposing CO_2 molecules clustering around carbonyl groups and interfering with the original hydrogen bonding network of the nonexpanded solvent.

In all the cases, we can also see that the viscosity variation when the CO_2 molar fraction is increased is more evident for the lowest temperatures. In other words, the slopes of the curves are more pronounced for low temperatures. This is an interesting behavior as for example the CO_2-expanded methyl acetate system, at 298.2 K, for a CO_2 molar fraction of 0.8, exhibits approximately 60% decreased viscosity, with only a 10% density decrease, just before the already mentioned abrupt decrease with x_{CO_2}.

Effect of the Modulation of Solvent Properties in Morphology of TiO_2 Microparticles. Porosity of materials is an important parameter when TiO_2 μPs are prepared as it greatly influences performances of the particles in catalysis, adsorption, reactivity, and so on. Additionally, solvent properties such as viscosity, polarity, and density strongly influences particle growth and coarsening mechanisms in materials preparation.

TiO_2 μPs were synthesized in CO_2 expanded ethyl and isoamyl acetates at 323.2, 353.2, or 373.2 K. For these temperatures, the values of π^* were obtained by extrapolating the data for other temperatures shown in the section Solvatochromic Determinations. Density and viscosity values were obtained by MD calculations in the same way as described in the section Solvatochromic Determinations of Materials and Methods.

Pore diameters and specific surface area obtained from BET analysis of the TiO_2 μPs are presented in Table S6, together with π^*, density, and viscosity of the CO_2-expanded alkyl acetates used in the synthesis. Figure 6 shows the effect of these parameters on specific surface area, and values are given in Table S6. Even though some dispersion is observed in the results, a clear trend can be observed concerning influence of density, π^*, and viscosity of the medium used for the synthesis. Previous studies have shown the strong influence of solvent properties on the morphological properties of properties. It has been observed, for example, that an increase in polarity of the solvent allows obtaining bigger crystals in SnO_2 nanoparticles (NPs), whereas the solvents of lower polarities induced smaller crystals. The optical band gap of SnO_2 increases with the polarity of the solvent as well.[19] For ZnO NPs, it has been shown that viscosity of the solvent strongly influences the rate constant of the growth kinetics; however, the dielectric constant of the solvent plays an important role as well, by solubilizing ZnO and influencing as well particle growth and coarsening.[20] SEM was used to confirm the morphology of the TiO_2 samples formed under biphasic conditions, in the GXL phase, and to compare these observations with the physical properties obtained by BET analysis. Microphotographs (Figure S5) show different morphologies obtained in the TIO_2 microparticles. As observed, a change in solvent parameters strongly influences the morphological properties observed by SEM. The sizes of crystals change with solvent parameters in ethyl and isoamyl acetates; however, antagonist effects can play a role in the growth of the particles, as in the case of viscosity where a decrease can favor growth kinetics, and in solvation properties, where a decrease can favor small particles obtaining as in ZnO particles.

From SEM microphotographs, it can be observed that samples (f), (g), (h), and (i), which are prepared with isoamyl acetate, presented the smallest particles (less than 1 μm), almost indiscernible at the magnification allowed by the equipment used.

From these results, it can be concluded that solubility and transport properties of the solvent environment have a great impact on the morphological properties of the particles obtained.

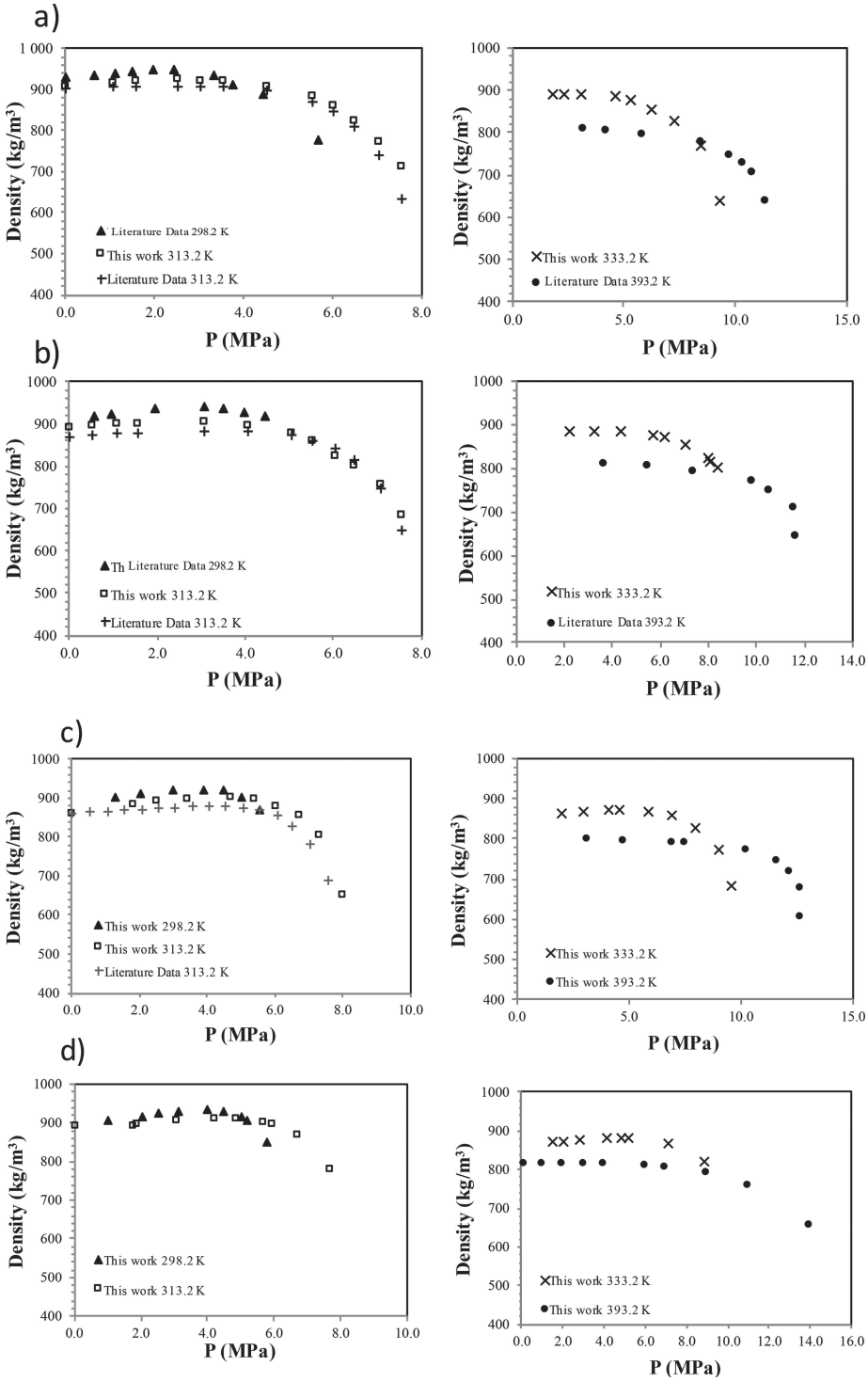

Figure 4. MD calculated density as a function of CO_2 pressure for (a) methyl, (b) ethyl, (c) propyl, and (d) isoamyl acetates expanded by CO_2. Literature data at 313.2K have been obtained experimentally. Literature data at 298.2 and 313.2 K for methyl and ethyl acetates (in figures a and b) were taken from ref 50 and represent MD results.

Morphological properties can then be modulated to optimize TiO_2-based materials which are essential to adapt optical, electrical, chemical, and magnetic properties of these materials for specific applications. Also, it can be said that GXLs are complex systems, where changes in pressure modifies simultaneously all the properties of the expanded phase, but not necessarily at the same scale. Discrimination of the effects of each one of these properties on chemical or physical processes happening in GXLs is thus difficult. In the case presented here, it is clear that properties of the expanded phase have an effect on the morphology of the particles generated; however, even if these effects are presented separately, it is probably the combination of the properties

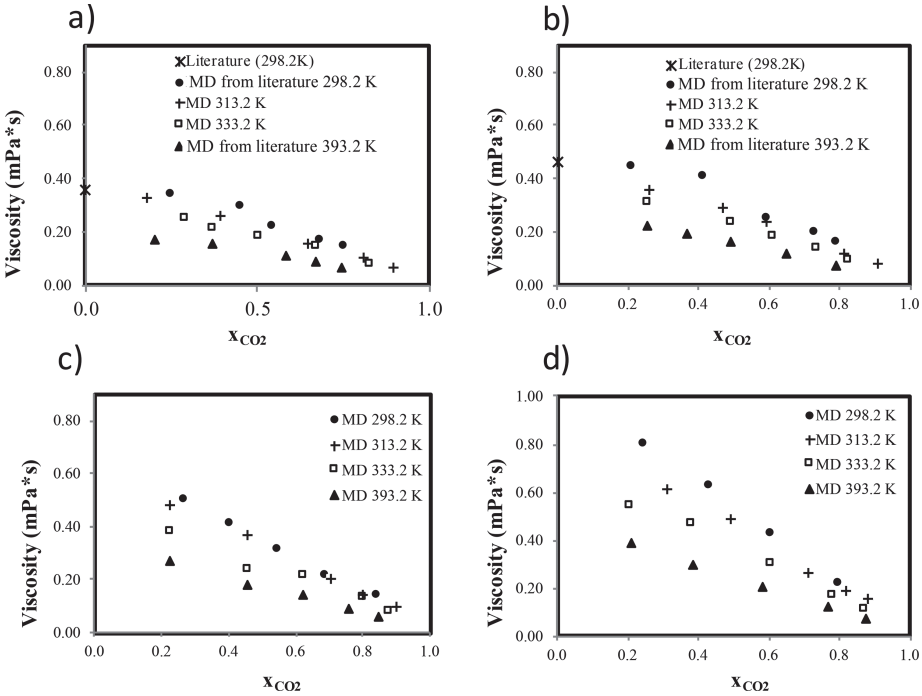

Figure 5. MD calculated viscosity (cP) as a function of CO_2 molar fraction in the expanded phase for (a) methyl, (b) ethyl, (c) propyl, and (d) isoamyl acetates expanded by CO_2. Literature data at 298.2 K has been obtained experimentally. MD results from literature at 298.2 and 313.2 K for methyl and ethyl acetates (in figures a and b) were taken from ref 50.

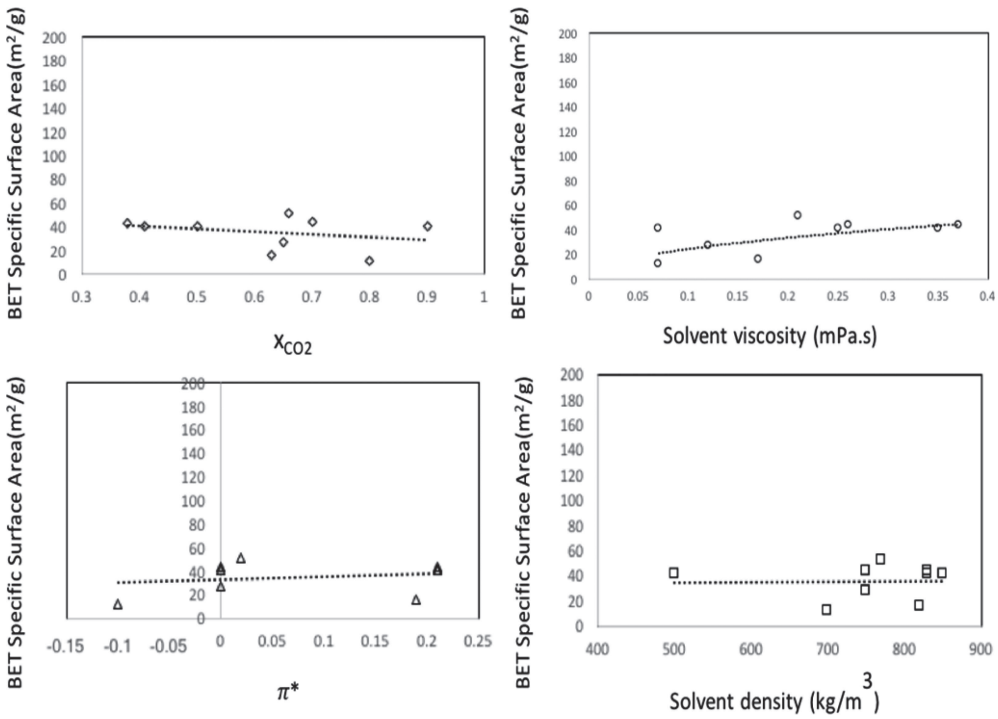

Figure 6. Effect of the modulation of the solvent properties on the morphologic properties of the TiO_2 particles obtained.

of the expanded phase that gives specific morphologic characteristics to the particles.

CONCLUSIONS

An extensive study involving experimental and numerical determinations has been carried out in order to characterize four alkyl acetates when expanded by CO_2. This study includes the experimental determination of the π^* parameter of the expanded phase together with density and viscosity obtained by MD methods.

The expansion phenomena and the associated changes in transport and solvation properties of the mixture were evaluated

in a range of temperatures from 298.2 to 393.2 K and pressures up to 160 bar.

Polarity was assessed through π^* Kamlet–Taft parameter determination using a solvatochromic method. It was shown that the expanded-phase properties can be widely modulated through CO_2 pressure. This variation is proportionally dependent on the presence of CO_2, which is intimately related to the nature of the solvent, the temperature, and the pressure. Thermochromism, which represents the effect of temperature on solvatochromic measurements, was taken into account and obtained values corrected accordingly.

Numerical determinations using Molecular Modeling were performed to obtain the CO_2-expanded-phase density and good agreement with experimental literature data was obtained at almost all the molar fractions values.

It was observed that modulation of physicochemical properties of the CO_2-expanded alkyl acetates used as solvents greatly influenced the morphological properties of TiO_2 particles. A decrease on BET pore diameter was clearly obtained with higher concentrations of CO_2, which means with pressure. This decrease was undoubtedly induced by changes in physicochemical properties of the solvent by CO_2, even if it is difficult to discriminate at this state the effect of each one of the properties separately, as CO_2 induces changes on all the properties of the expanded phase simultaneously. It is, however, very probable that the combination of the properties of the expanded phase gives specific morphologic characteristics to the particles.

This example shows that GXLs can be a great means to achieve the modulation of pore diameter size of TiO_2 nanoparticles, which is essential to control optical, electrical, chemical, and magnetic properties of these nanoparticles for specific applications such as catalysis, formulation, and so on.

As shown in this study, rational control of the properties of GXLs may allow great adaptability and optimization of chemical processes. This study represents an effort to help in the rational application of these systems in chemical processes

■ ASSOCIATED CONTENT

Supporting Information

The Supporting Information is available free of charge on the ACS Publications website at DOI: 10.1021/acssuschemeng.8b00454.

Molecular modeling typical box; normalized absorbance spectra of Nile Red in CO_2-expanded ethyl acetate at different pressures; thermochromism on NR absorption wavelength in neat alkyl acetates; packing fraction as a function of CO_2 composition for the alkyl acetates studied; SEM images of TiO_2 anatase synthesized in CO_2-expanded ethyl and isoamyl acetates; Amber Cornell Extended Force field bond and pairwise potentials; Amber Cornell Extended Force field bond and pairwise potentials; fitted atomic center charges for the alkyl acetates molecules studied; corrected Kamlet–Taft π^* values for methyl, ethyl, propyl, and isoamyl acetates; values of π^* for some current organic solvents; density values obtained from Molecular Dynamics for CO_2-expanded systems; and specific surface area and pore diameter obtained from BET for the TiO_2 microparticles synthesized (PDF)

■ AUTHOR INFORMATION

Corresponding Author

*E-mail: yaocihuatl.medinagonzalez@ensiacet.fr. Tel.: +33 (0)5 3432 3679.

ORCID

Yaocihuatl Medina-Gonzalez: 0000-0003-2859-8158

Notes

The authors declare no competing financial interest.

■ ACKNOWLEDGMENTS

The authors are grateful to financial support from Natural Sciences and Engineering Research Council of Canada (NSERC) Discovery and Strategic Programs, from the French Ministry for Higher Education and Research and from the France Canada Research Fund program. Iréa Touche, Fouad Oulebsir and Guillaume Galliero are deeply thanked for their help during LAMMPS utilization as well as the Calcul en Midi-Pyrénees (CALMIP) for the access to the EOS supercomputer under the allocations P1535 and P1526.

■ REFERENCES

(1) West, K. N.; Hallett, J. P.; Jones, R. S.; Bush, D.; Liotta, C. L.; Eckert, C. A. CO_2-Induced Miscibility of Fluorous and Organic Solvents for Recycling Homogeneous Catalysts. *Ind. Eng. Chem. Res.* **2004**, *43* (16), 4827–4832.

(2) Lu, J.; Lazzaroni, M. J.; Hallett, J. P.; Bommarius, A. S.; Liotta, C. L.; Eckert, C. A. Tunable Solvents for Homogeneous Catalyst Recycle. *Ind. Eng. Chem. Res.* **2004**, *43* (7), 1586–1590.

(3) Jessop, P. G.; Subramaniam, B. Gas-expanded liquids. *Chem. Rev.* **2007**, *107* (6), 2666–2694.

(4) Ford, J. W.; Lu, J.; Liotta, C. L.; Eckert, C. A. Solvent Effects on the Kinetics of a Diels-Alder Reaction in Gas-Expanded Liquids. *Ind. Eng. Chem. Res.* **2008**, *47* (3), 632–637.

(5) Soh, L.; Chen, C.-C.; Kwan, T. A.; Zimmerman, J. B. Role of CO_2 in Mass Transfer, Reaction Kinetics, and Interphase Partitioning for the Transesterification of Triolein in an Expanded Methanol System with Heterogeneous Acid Catalyst. *ACS Sustainable Chem. Eng.* **2015**, *3* (11), 2669–2677.

(6) Konovalov, A. I.; Breus, I. P.; Sharagin, I. A.; Kiselev, V. D. Solvation Effects in Diels-Alder Reaction of 4-Phenyl-1,2,4-triazoline-3,5-dione with Anthracene and Trans,trans-1,4-diphenyl-1,3-butadiene. *Zhurnal Org. Khimii* **1979**, *15* (2), 361–367.

(7) Burrage, M. E.; Cookson, R. C.; Gupte, S. S.; Stevens, I. D. R. Substituent and solvent effects on the Diels–Alder reactions of triazolinediones. *J. Chem. Soc., Perkin Trans. 2* **1975**, *0* (12), 1325–1334.

(8) Thompson, R. L.; Gläser, R.; Bush, D.; Liotta, C. L.; Eckert, C. A. Rate Variations of a Hetero-Diels–Alder Reaction in Supercritical Fluid CO_2. *Ind. Eng. Chem. Res.* **1999**, *38* (11), 4220–4225.

(9) Siougkrou, E.; Galindo, A.; Adjiman, C. S. On the optimal design of gas-expanded liquids based on process performance. *Chem. Eng. Sci.* **2014**, *115*, 19–30.

(10) Moity, L.; Durand, M.; Benazzouz, A.; Pierlot, C.; Molinier, V.; Aubry, J.-M. Panorama of sustainable solvents using the COSMO-RS approach. *Green Chem.* **2012**, *14* (4), 1132.

(11) Kamlet, M. J.; Taft, R. W. The solvatochromic comparison method. I. The.beta.-scale of solvent hydrogen-bond acceptor (HBA) basicities. *J. Am. Chem. Soc.* **1976**, *98* (2), 377–383.

(12) Wyatt, V. T.; Bush, D.; Lu, J.; Hallett, J. P.; Liotta, C. L.; Eckert, C. A. Determination of solvatochromic solvent parameters for the characterization of gas-expanded liquids. *J. Supercrit. Fluids* **2005**, *36* (1), 16–22.

(13) Marcus, Y. The properties of organic liquids that are relevant to their use as solvating solvents. *Chem. Soc. Rev.* **1993**, *22* (6), 409–416.

(14) Sigman, M. E.; Lindley, S. M.; Leffler, J. E. Supercritical carbon dioxide: behavior of.pi.* and.beta. solvatochromic indicators in media of different densities. *J. Am. Chem. Soc.* **1985**, *107* (6), 1471–1472.

(15) Fermi, I. E.; Pasta, P.; Ulam, S.; Tsingou, M. *Studies of the Nonlinear Problems*; Los Alamos Scientific Laboratory of the University of California: Berkeley, CA, 1955.

(16) Alder, B. J.; Wainwright, T. E. Studies in Molecular Dynamics. *J. Chem. Phys.* **1959**, *31* (2), 459–466.

(17) Rahman, A. Correlations in the Motion of Atoms in Liquid Argon. *Phys. Rev.* **1964**, *136* (2A), A405−A411.
(18) Zhong, H.; Lai, S.; Wang, J.; Qiu, W.; Lüdemann, H.-D.; Chen, L. Molecular Dynamics Simulation of Transport and Structural Properties of CO_2 Using Different Molecular Models. *J. Chem. Eng. Data* **2015**, *60* (8), 2188−2196.
(19) Kumar, V.; Singh, K. K.; Kumar, A.; Kumar, M.; Singh, K. K.; Vij, A.; Thakur, A. Effect of solvent on crystallographic, morphological and optical properties of SnO_2 nanoparticles. *Mater. Res. Bull.* **2017**, *85*, 202−208.
(20) Hu, Z.; Oskam, G.; Searson, P. C. Influence of solvent on the growth of ZnO nanoparticles. *J. Colloid Interface Sci.* **2003**, *263*, 454−460.
(21) Hoang, H. N.; Granero-Fernandez, E.; Yamada, S.; Mori, S.; Kagechika, H.; Medina-Gonzalez, Y.; Matsuda, T. Modulating Biocatalytic Activity toward Sterically Bulky Substrates in CO_2-Expanded Biobased Liquids by Tuning the Physicochemical Properties. *ACS Sustainable Chem. Eng.* **2017**, *5* (11), 11051−11059.
(22) Kato, M.; Sugiyama, K.; Sato, M.; Kodama, D. Volumetric property for carbon dioxide + methyl acetate system at 313.15K. *Fluid Phase Equilib.* **2007**, *257* (2), 207−211.
(23) Wagner, Z.; Pavlíček, J. Vapour-liquid equilibrium in the carbon dioxide-ethyl acetate system at high pressure. *Fluid Phase Equilib.* **1994**, *97*, 119−126.
(24) Aida, T.; Aizawa, T.; Kanakubo, M.; Nanjo, H. Analysis of volume expansion mechanism of CO_2-acetate systems at 40 °C. *J. Supercrit. Fluids* **2010**, *55* (1), 56−61.
(25) Cheng, C. H.; Chen, Y. P. Vapor-liquid equilibria of carbon dioxide with isopropyl acetate, diethyl carbonate and ethyl butyrate at elevated pressures. *Fluid Phase Equilib.* **2005**, *234* (1−2), 77−83.
(26) Sima, S.; Feroiu, V.; Geană, D. New high pressure vapor-liquid equilibrium data and density predictions for carbon dioxide+ethyl acetate system. *Fluid Phase Equilib.* **2012**, *325*, 45−52.
(27) Kwon, C. H.; Seo, M. Do; Kim, S. W.; Lee, C. S.; Kang, J. W. Vapor - Liquid equilibrium for carbon dioxide + isopropyl, isobutyl, and isoamyl acetates. *J. Chem. Eng. Data* **2007**, *52* (3), 727−730.
(28) Smith, R. L.; Yamaguchi, T.; Sato, T.; Suzuki, H.; Arai, K. Volumetric behavior of ethyl acetate, ethyl octanoate, ethyl laurate, ethyl linoleate, and fish oil ethyl esters in the presence of supercritical CO_2. *J. Supercrit. Fluids* **1998**, *13* (1−3), 29−36.
(29) Falco, N.; Kiran, E. Volumetric properties of ethyl acetate + carbon dioxide binary fluid mixtures at high pressures. *J. Supercrit. Fluids* **2012**, *61*, 9−24.
(30) Tian, Y. L.; Zhu, H. G.; Xue, Y.; Liu, Z. H.; Yin, L. Vapor-liquid equilibria of the carbon dioxide + ethyl propanoate and carbon dioxide + ethyl acetate systems at pressure from 2.96 to 11.79 MPa and temperature from 313 to 393 K. *J. Chem. Eng. Data* **2004**, *49* (6), 1554−1559.
(31) Byun, H.-S.; Choi, M.-Y.; Lim, J.-S. High-pressure phase behavior and modeling of binary mixtures for alkyl acetate in supercritical carbon dioxide. *J. Supercrit. Fluids* **2006**, *37*, 323−332.
(32) Ohgaki, K.; Katayama, T. Isothermal vapor-liquid equilibriums for systems Ethyl Ether-Carbon Dioxide and Methyl Acetate-Carbon Dioxide at High Pressures. *J. Chem. Eng. Data* **1975**, *20* (3), 264−267.
(33) Kamlet, M. J.; Abboud, J. L.; Taft, R. W. The solvatochromic comparison method. 6. The.pi.* scale of solvent polarities. *J. Am. Chem. Soc.* **1977**, *99* (18), 6027−6038.
(34) Kamlet, M. J.; Abboud, J. L. M.; Abraham, M. H.; Taft, R. W. Linear solvation energy relationships. 23. A comprehensive collection of the solvatochromic parameters,.pi.*,.alpha., and.beta., and some methods for simplifying the generalized solvatochromic equation. *J. Org. Chem.* **1983**, *48* (17), 2877−2887.
(35) Taft, R. W.; Kamlet, M. J. The solvatochromic comparison method. 2. The.alpha.-scale of solvent hydrogen-bond donor (HBD) acidities. *J. Am. Chem. Soc.* **1976**, *98* (10), 2886−2894.
(36) Ford, J. W. *Designing for sustainability with CO_2-tunable solvents*. Ph.D. Thesis, Georgia Institute of Technology, 2007.
(37) Ford, J. W.; Janakat, M. E.; Lu, J.; Liotta, C. L.; Eckert, C. A. Local polarity in CO_2-expanded acetonitrile: A nucleophilic substitution reaction and solvatochromic probes. *J. Org. Chem.* **2008**, *73* (9), 3364−3368.
(38) Li, H.; Arzhantsev, S.; Maroncelli, M. Solvation and solvatochromism in CO_2-expanded liquids. 2. Experiment-simulation comparisons of preferential solvation in three prototypical mixtures. *J. Phys. Chem. B* **2007**, *111* (12), 3208−3221.
(39) Scurto, A. M.; Hutchenson, K.; Subramaniam, B. Gas-Expanded Liquids: Fundamentals and Applications. *Gas-Expanded Liquids and Near-Critical Media*; ACS Symposium Series; American Chemical Society: Washington, DC, 2009; Vol. *1006*, pp 1−3. DOI: 10.1021/bk-2009-1006.ch001.
(40) Medina-Gonzalez, Y.; Jarray, A.; Camy, S.; Condoret, J.-S.; Gerbaud, V. CO_2-Expanded Alkyl Lactates: A Physicochemical and Molecular Modeling Study. *J. Solution Chem.* **2017**, *46* (2), 259−280.
(41) Gohres, J. L.; Kitchens, C. L.; Hallett, J. P.; Popov, A. V.; Hernandez, R.; Liotta, C. L.; Eckert, C. A. A spectroscopic and computational exploration of the cybotactic region of gas-expanded liquids: methanol and acetone. *J. Phys. Chem. B* **2008**, *112* (15), 4666−4673.
(42) Deye, J. F.; Berger, T. A.; Anderson, A. G. Nile Red as a Solvatochromic Dye for Measuring Solvent Strength in Normal Liquids and Mixtures of Normal Liquids with Supercritical and Near Critical Fluids. *Anal. Chem.* **1990**, *62* (6), 615−622.
(43) Kurniasih, I. N.; Liang, H.; Mohr, P. C.; Khot, G.; Rabe, J. P.; Mohr, A. Nile Red Dye in Aqueous Surfactant and Micellar Solution. *Langmuir* **2015**, *31* (9), 2639−2648.
(44) Mistry, R. *Characterisation and Applications of CO_2-Expanded Solvents*. Ph.D. Thesis, University of Leicester, 2008.
(45) Abbott, A. P.; Hope, E. G.; Mistry, R.; Stuart, A. M. Probing the structure of gas expanded liquids using relative permittivity, density and polarity measurements. *Green Chem.* **2009**, *11* (10), 1530−1535.
(46) Soave, G.; Progetti, S.; Sviluppo, D. Equilibrium constants from a modified Redkh-Kwong equation of state. *Chem. Eng. Sci.* **1972**, *27*, 1197−1203.
(47) Boston, J. F.; Mathias, P. M. Phase equilibria in a third-generation process simulator *Proceedings of the 2nd International Conference on Phase Equilibria and Fluid Properties in the Chemical Process Industries*, West Berlin, March 17−21, 1980; pp 823−849.
(48) Scienomics. *Materials and Process Simulation (MAPS)*, 2017. See the following: http://www.scienomics.com/software/.
(49) Sandia National Laboratories. *Large Atomic/Molecular Massively Parallel Simulator (LAMMPS)*, 1995. See the following: http://lammps.sandia.gov/.
(50) Granero-Fernandez, E.; Condoret, J.-S.; Gerbaud, V.; Medina-Gonzalez, Y. Molecular Dynamics Simulations of Gas-Expanded Liquids. In *27th European Symposium on Computer Aided Process Engineering*; Espuña, A., Graells, M., Puigjaner, L., Eds; Elsevier: Amsterdam, 2017; Vol. *40*, pp 175−180. DOI: 10.1016/B978-0-444-63965-3.50031-3
(51) Kubo, R. The fluctuation-dissipation theorem. *Rep. Prog. Phys.* **1966**, *29* (1), 255.
(52) Green, M. S. Markoff Random Processes and the Statistical Mechanics of Time-Dependent Phenomena. II. Irreversible Processes in Fluids. *J. Chem. Phys.* **1954**, *22* (3), 398−413.
(53) Kubo, R. Statistical-Mechanical Theory of Irreversible Processes. I. General Theory and Simple Applications to Magnetic and Conduction Problems. *J. Phys. Soc. Jpn.* **1957**, *12* (6), 570−586.
(54) Frisch, M. J.; Trucks, G. W.; Schlegel, H. B.; Scuseria, G. E.; Robb, M. A.; Cheeseman, J. R.; Scalmani, G.; Barone, V.; Mennucci, B.; Petersson, G. A.; et al.. *Gaussian 09*; Gaussian, Inc.: Wallingford CT. 2016.
(55) Singh, U. C.; Kollman, P. A. An approach to computing electrostatic charges for molecules. *J. Comput. Chem.* **1984**, *5* (2), 129−145.
(56) Besler, B. H.; Merz, K. M.; Kollman, P. A. Atomic charges derived from semiempirical methods. *J. Comput. Chem.* **1990**, *11* (4), 431−439.
(57) Wagner, Z. Vapour-liquid equilibrium at high pressure in the system containing carbon dioxide and propyl acetate. *Fluid Phase Equilib.* **1995**, *110* (1−2), 175−182.

(58) Schwinghammer, S.; Siebenhofer, M.; Marr, R. Determination and modelling of the high-pressure vapour-liquid equilibrium carbon dioxide-methyl acetate. *J. Supercrit. Fluids* **2006**, *38* (1), 1–6.
(59) Da Silva, M. V.; Barbosa, D.; Ferreira, P. O.; Mendonça, J. High pressure phase equilibrium data for the systems carbon dioxide/ethyl acetate and carbon dioxide/isoamyl acetate at 295.2, 303.2 and 313.2 K. *Fluid Phase Equilib.* **2000**, *175* (1–2), 19–33.
(60) Sackett, D. L.; Wolff, J. Nile red as a polarity-sensitive fluorescent probe of hydrophobic protein surfaces. *Anal. Biochem.* **1987**, *167* (2), 228–234.
(61) Ghanadzadeh Gilani, A.; Moghadam, M.; Zakerhamidi, M. S. Solvatochromism of Nile red in anisotropic media. *Dyes Pigm.* **2012**, *92* (3), 1052–1057.
(62) Golini, C. M.; Williams, B. W.; Foresman, J. B. Further Solvatochromic, Thermochromic, and Theoretical Studies on Nile Red. *J. Fluoresc.* **1998**, *8* (4), 395.
(63) Li, H.; Maroncelli, M. Solvation and Solvatochromism in CO_2-Expanded Liquids. 1. Simulations of the Solvent Systems CO_2 + Cyclohexane, Acetonitrile, and Methanol. *J. Phys. Chem. B* **2006**, *110*, 21189. (b) Cunico, L.; Turner, C. Supercritical fluids and gas expanded liquids. In *The application of green solvents in separation processes*, 1st ed.; Pena-Pereira, F., Tobiszewski, M., Eds.; Elsevier: Amsterdam, DOI: 10.1016/B978-0-12-805297-6.00007-3.
(64) Bondi, A. van der Waals Volumes and Radii. *J. Phys. Chem.* **1964**, *68* (3), 441–451.
(65) Dysthe, D. K.; Fuchs, A. H.; Rousseau, B. Prediction of fluid mixture transport properties by molecular dynamics. *Int. J. Thermophys.* **1998**, *19*, 437–448.